

Deep learning approach to structural performance prediction of tall buildings in seismic areas

Pooyan KAZEMI^{*,a}, Michela TURRIN^b, Charalampos ANDRIOTIS^b,
Alireza ENTEZAMI^a, Aldo GHISI^a, Stefano MARIANI^a

^a Department of Civil and Environmental Engineering, Politecnico di Milano
Piazza Leonardo da Vinci 32, 30133, Milano, Italy

*seyedpooyan.kazemi@polimi.it

^b Architectural Engineering and Technology Department, Delft University of Technology
Julianalaan 134, 2628 BL, Delft, The Netherlands

Abstract

To study the interplay between architectural form and seismic response in tall buildings with outer diaphragms during the early design phase, advanced computational analysis and artificial intelligence methods are adopted. Dynamic numerical simulations of moderate magnitude earthquakes are performed, investigating different architectural forms to inform early design decisions within an extensive design space. Parametric design software, e.g. Rhinoceros, Grasshopper, is considered together with OpenSees. The numerical analysis evaluates the response to vertical static loads and lateral seismic excitations, in terms of inter-storey drifts, displacements and various stress metrics, under seven ground motion scenarios, using a dataset of 1000 tall buildings selected through Latin hypercube sampling. A multi-input multi-output feed-forward neural network is developed for this purpose; fine-tuning parameters such as network architecture, learning rate, batch size, and validation techniques enable the model to achieve a low validation loss, indicating an effective learning process. Designers can take advantage of the workflow applied to the database to guide their early decisions.

Keywords: AI-enhanced design, deep learning, tall building optimization, architectural form generation, seismic simulation, surrogate modeling

1. Introduction

Several computational tools are now available to assist designers in the early stages of form finding, from parametric design software to structural analysis simulators [1]. With emphasis on the interaction between form and structural behaviour, the category of tall buildings with outer diaphragms is considered in this work [2]. In such structures, the designer can be inspired by many alternative solutions, and issues may arise when dealing with a large amount of data to discriminate interesting designs defined by high-dimensional information, as discussed e.g. in [3]. Harnessing artificial intelligence (AI) capabilities can be useful for this purpose [4, 5], but the framework should allow efficient solutions in terms of computational effort. In the past, AI tools proved good to predict and assess the structural performance, either from numerical or experimental data, see e.g. [6, 7], but rarely they have been used to guide decisions in the early design, when the alternatives at disposals expand enormously the design space [8, 9]. Recent reviews on the application of AI to structural performance prediction have focused on structural members or construction details such as joints [10] or ground motion parameters and frame design parameters for buildings with regular or assumed geometry [11]. On the other hand, significant efforts have been

made on the architectural side to generate new forms from existing ones, also using deep learning tools, see e.g. [12]. Of course, the convergence of the structural and architectural experiences also points to a desirable higher level of collaboration in the early design phase, an AI-based application niche that has been less explored so far.

However, in the early design phase, generating and managing large datasets with thousands of results can be challenging: therefore, in this work, extending what already shown for small datasets [8, 9], we aim to provide a workflow to discriminate between architectural options in view of their structural outcome. Here, a significant increase in dataset dimension with respect to our previous works is considered, together with dynamic simulations of tall buildings with outer diagrids subjected to moderate earthquakes [2, 13]. A multi-input multi-output feed-forward neural network (MIMO-FNN) [14] is adopted as a surrogate model [15], to achieve the goal of inspect and sort the models in the database to help the designer's choice. The low losses of the training/validation tests confirm the validity of the proposed approach.

2. Design space: architectural forms and structural analysis

A dataset consisting of 1,000 tall building models featuring various vertical transformation methods, including tapered, twisted, and curvilinear forms, has been created. The design space has been defined by choosing the following architectural parameters (also shown in Table 1): top plan geometry side count (X1), bottom plan geometry side count (X2), top and bottom plan orientation (X3), number of stories (X4), floor-to-floor height (X5), vertical transformation method (X6), tapering (X7), twisting angle (X8), curvilinear location of control floor (X9), and curvilinear scale of control floor (X10). The interdependencies among these parameters, especially the influence of the vertical transformation method (X6) on parameters X7 to X10, are relevant: for instance, in models with a tapered form, parameters X8 to X10 are not applicable. The conditional relationships between these variables are indicated in the first column of Table 1.

The computational burden of numerical simulations to compute the structural response on such a set of models needs a careful consideration of the dataset size. The potential for expanding the variables is vast; however, performing detailed architectural and structural modelling within computationally limited resources requires a judicious reduction in the number of models. From an initial exploration that identified up to 370,000 feasible variations, the selection process has chosen 61,200 solutions obtained by assigning the X1-X10 values listed in last column of Table 1. This selection is such that a balanced representation across the different variables is achieved, preventing dataset imbalances that could skew the design space. For example, ensuring that the number of possibilities for tapering, twisting, and curvilinear transformations are proportionally represented is essential for a balanced dataset. The final dataset includes a wide range of possibilities, from simple straight forms to more complex geometries, as shown in Figure 1.

To better understand the vertical transformation methods employed in the architectural models, the parameter effects are illustrated in Figure 2. Specifically, for the tapering transformation, X7 quantifies the tapering intensity. A value of 50% characterises a highly tapered form, where the top plan is scaled down to 50%, whereas a value of 100% corresponds to no tapering. Regarding twisting transformations, X8 represents the rotational angle of the top plan relative to the bottom plan. The minimal twisting is achieved at a 30° angle, and the maximum twisting is represented by a 90° angle. Regarding curvilinearity, X9 determines the position of the control floor, which defines the curvilinearity location within the building height: this control floor can be positioned in the first, second, or third quarter of the building total height. X10 specifies the intensity of the curvilinearity by scaling the control floor plan: a scale factor of 0.85 indicates a concave curvilinearity, whereas 1.15 stands for convex curvilinearity, as depicted

in Figure 3.

Table 1: Design space and parameters that define the architectural modelling of tall buildings with outer diagrids, as considered in this work.

Condition	Parameter	Name	Description	Cardinality	Values
	X1	Top plan geometry side count	Number of edges of the top plan geometry	10	[3,4,...,12]
	X2	Bottom plan geometry side count	Number of edges of the bottom plan geometry	10	[3,4,...,12]
	X3	Top and bottom plan orientation	Relative position of top and bottom plan with respect to each other (corner to corner =0, corner to edge =1)	2	[0,1]
	X4	Number of stories	Total number of floors	6	[40,44,48,...,60]
	X5	Floor height	Distance between two consecutive floors (m)	3	[3.5,4,4.5]
	X6	Vertical transformation method	How top and bottom plan connected together (tapered/twisted/curvilinear)		[0,1,2]
If X6=0	X7	Tapering	Scale factor of the area of top plan compared to bottom plan	6	[50%,60%,...,90%, 100%]
If X6=1	X8	Twisting angle	Angle that the top plan is rotated (°)	5	[30,45,60,75,90]
If X6=2	X9	Curvilinear location of control floor	Parameter to define the position of curvilinearity	3	[0.25,0.5,0.75]
	X10	Curvilinear; scale of control floor	Parameter to define the intensity of curvilinearity	2	[0.85,1.15]
Total solutions				61,200	

Since tall buildings are characterized by a varying number of stories, the area proportionality of the core to the building's height is crucial. This area, housing vital functions such as the vertical transportation and mechanical systems, needs to be scaled according to the number of floors; buildings with more stories require a larger core. Unpublished work by Gokce et al., which surveyed core areas in a broad spectrum of tall buildings, has served as the reference for our analysis. A linear relationship for core ratios across different heights, implemented in Grasshopper to define the core ratio for each model (19.3% for 140 m height based on five buildings, and 23.8% for 270 m height based on seven buildings), has been implemented. The core geometry for all models has been standardized to a dodecagon, ensuring uniformity in structural analysis and making possible a comparison of the performances.

To reduce the computational burden, 1000 models out of 61,200 solutions have been chosen through a Latin hypercube sampling through the pyDOE2 Python library. These samples are then mapped to the actual parameter ranges, with subsequent validation to ensure a well-distributed sample set within the design space. The 1000 tall building models have been obtained with the Colibri plugin, fed with the X1-X10 variables. Structural models and a (Python) file containing seismic simulation data, among other necessary information for post-processing, have been then produced within an automated procedure. For each model, a picture is generated and the model information is documented in a CSV file.

OpenSees is used for finite element dynamic simulations [16]. The plugin Alpaca 4D has been adapted to create Python scripts for execution in OpenSeesPy. The Delft high-performance computer is used to produce 7000 simulations, since each of the 1000 models is subjected to 7 earthquakes, obtained from the NGA-West2 database via the PEER ground motion online tool [17]. An excitation along two horizontal orthogonal directions has been imposed at the base of the tall buildings.

Time histories of lateral displacements, velocities and accelerations are recorded for relevant points at each floor. In addition, as a diaphragm constraint is imposed on the nodes at each floor, the same quantities are also stored at the constraint reference node. Reaction forces at the restrained nodes at the building

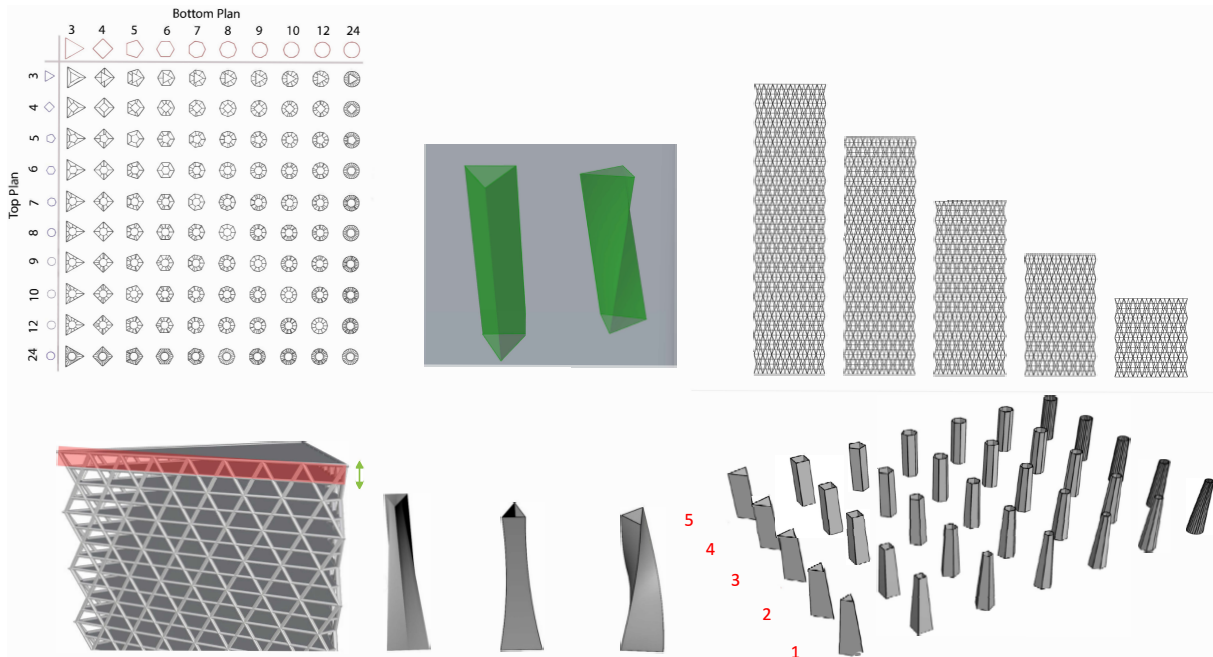


Figure 1: Visualization of the parameters considered in this work. Top line: (left) top and bottom plan geometry side count (X1, X2); (middle) top and bottom plan orientation (X3); (right) number of stories (X4). Bottom line: (left) floor height (X5); (middle) vertical transformation method (X6); (right) tapering, with models 5 without tapering and models 1 with the highest tapering (X7).

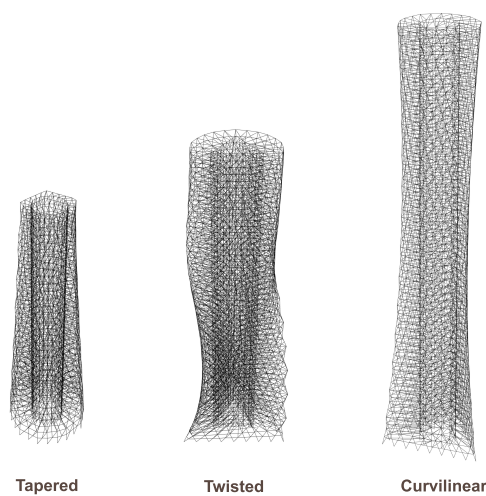


Figure 2: Visualization of the tapered/twisted/curvilinear transformation (X6=0/1/2).

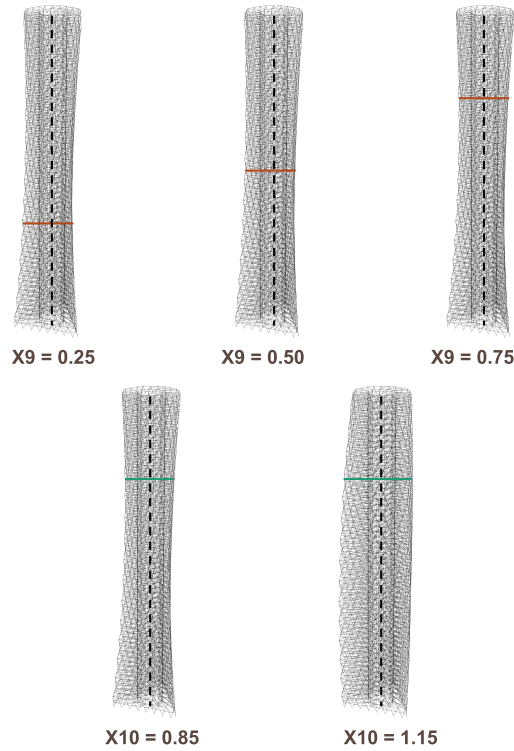


Figure 3: Visualization of the curvilinear transformation. Top line: X9 defines the position of curvilinearity, from 0 (bottom floor) to 1 (top floor). Bottom line: X10 defines the intensity of curvilinearity, e.g. (left) X10 = 0.85, (right) X10 = 1.15.

base are included in the output as well, together with internal forces and stresses for relevant elements in the outer diagrid and core. Additionally, inter-story drifts are computed during post-processing, since they are important in assessing the building's performance [18]. A Python script has been utilized to systematically process files containing data on overall acceleration, displacement, inter-story drift, stress in diagrids, total stress, torsion, and overall reactions for each model across all ground motion scenarios. Moreover, additional responses in terms of economic and environmental (i.e. carbon footprint) costs have been derived from the building characteristics.

3. Surrogate modelling

A MIMO-FNN, whose architecture scheme is shown in Figure 4, has been tailored for the simultaneous prediction of the multiple structural responses to different inputs, after the training with the database described above.

A multi-input layer architecture, opposed to a traditional single-layer of inputs, is adopted here, to process variable types of inputs, namely building characteristics and ground motion features, to capture their separate impact on structural responses. Similarly, structural, environmental, and geometry-dependent responses have been considered independent and different layers in the network have been defined for each set of responses. To enhance the accuracy even further within the structural responses layer, a discretization process can be applied. For instance, a set of responses concerning inter-storey drift is independent from a set that represents acceleration: distinct output layers are hence used for the two sets. Nevertheless, although the inputs and outputs are organized into distinct layers to reflect the diversity of data types, e.g. they vary from building features to ground motion characteristic, the core architecture of the neural network model remains unique.

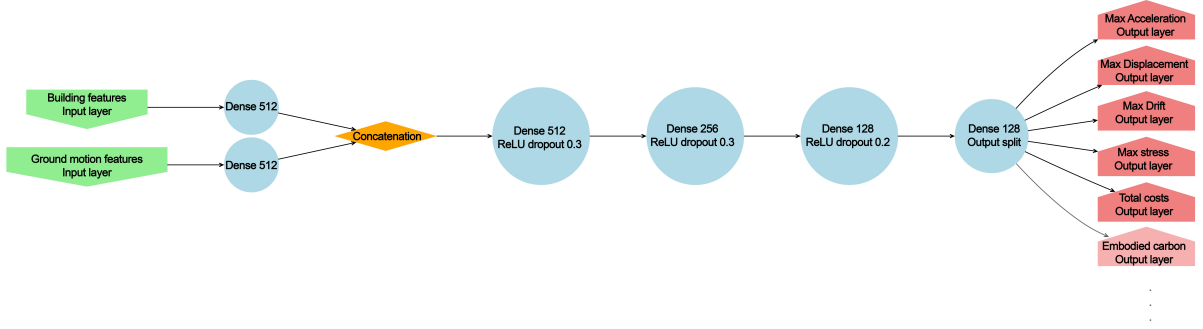


Figure 4: Scheme of the MIMO-FNN architecture.

MIMO-FNNs can discern the intricate relationships between diverse response groups, especially those derived from finite element simulations. Through the adjustment of the weights during the training phase, achieved via back-propagation and optimization algorithms such as Adam, these networks capture the patterns and correlations within the dataset; however, their proficiency is anchored in statistical learning, and therefore they lack of a conceptual understanding of the underlying physical phenomena. Thus, integrating domain knowledge into the model’s design, training, and validation processes is indispensable for ensuring that predictions are both statistically valid and meaningful from the engineering point of view.

The considered MIMO-FNN consists of dense layers with 512-256-128 neurons, respectively, and rectified linear unit (ReLU) activation functions. Dropout rates are set to 0.3/0.2/0.2 for each layer, respectively. The hyperparameters for the MIMO-FNN are collected in Table 2.

Table 2: Hyperparameters for the MIMO-FNN.

Hyperparameter	Value/description
Number of layers	Input, three hidden, output
Neurons per hidden layer	512, 256, 128
Activation function	ReLU
Loss function	RMSE
Batch size	32
Learning rate	2×10^{-5}
Weight decay	1×10^{-4}
Training epochs	100
Optimizer	Adam
Dropout rate	0.3, 0.3, 0.2

The root mean squared error (RMSE) loss, defined as

$$\text{Overall RMSE loss} = \sqrt{\frac{1}{N} \sum_{i=1}^N (\text{predicted_value}_i - \text{actual_value}_i)^2} \quad (1)$$

and computed across all the output features of the MIMO-FNN, encapsulates the model’s collective predictive performance. In Equation (1), N is the total number of data points (designs); predicted_value_i denotes the model prediction for the i -th data point; and actual_value_i represents the respective value from the simulator.

The overall workflow includes cross-validation (C-V) and subsequent retraining. It can be summarised

as follows.

1. Loading the pre-processed feature data and responses into the network input layer.
2. Partitioning into training and testing sets with 2–5 folds for C-V.
3. Executing the C-V for every fold; the training is carried out with a fixed number of epochs (100); the training/validation losses are inspected.
4. Averaging of losses post C-V, establishing a baseline for the final model retraining.
5. Final model iteration and model's evaluation on the whole test set.

In an optimal learning scenario, both training and validation losses exhibit a downward trajectory over epochs, ultimately converging to a low value. This pattern signifies that the MIMO-FNN not only learns effectively from the training dataset but also demonstrates good generalization capabilities on the validation dataset. Such convergence at low loss values is indicative of a model that balances learning and generalization without succumbing to overfitting or underfitting.

The examination of learning curves across an expanded cross-validation setup, increasing the number of folds from 2 to 5, aims to investigate potential improvements in model learning and generalization. Despite this adjustment, the anticipated significant enhancement in model performance has not been observed, underscoring the robust initial configuration of the MIMO-FNN.

The model performance, as reported by the RMSE evolutions shown in Figure 5, reveals a consistent decline in both training and validation RMSE values across epochs, indicative of effective learning and generalization. The absence of marked overfitting or underfitting, alongside the low final test RMSE, underscores the model's precise predictive accuracy. Moreover, the stability of performance across C-V folds highlights the MIMO-FNN's reliability and robustness in learning.

In summary, the MIMO-FNN showcases good performance, characterized by low RMSE values across training, validation, and testing phases. The learning curve visualization not only facilitates the monitoring of the model's learning trajectory but also substantiates the model's adeptness at capturing underlying patterns within the data.

To visualize and investigate the various tall building models in the database, Design Explorer is employed, a web application used to inspect multidimensional design spaces. Figure presents, in the top row, a selection of the features and responses adopted during the training of the MIMO-FNN. On the left side, features (in black colour), including building attributes (X1–X10 for a certain ground motion, are displayed. Meanwhile, the right side showcases eight out of the 91 (considered) structural simulation responses, encompassing e.g. maximum overall acceleration, displacement, inter-story drift, von Mises stress, torsion, base shear force, base bending moment, and total building mass.

The bottom row visually represents the building models: on the left, the model with the lowest average normalized response, and at the center the one with the highest average normalized response. Accompanying the images are the relevant values of features and responses. On the right, smaller images represent some of the other building models.

It is worth noting that the buildings are sorted based on the average normalized response for this exemplary visualization, although any other response could be utilized. Notably, the model with the lowest value features a curvilinear shape with 3-sided and 6-sided polygons as top and bottom plans respectively, while the model with the highest value also exhibits a curvilinear design with 9-sided and 4-sided polygons as top and bottom plans.

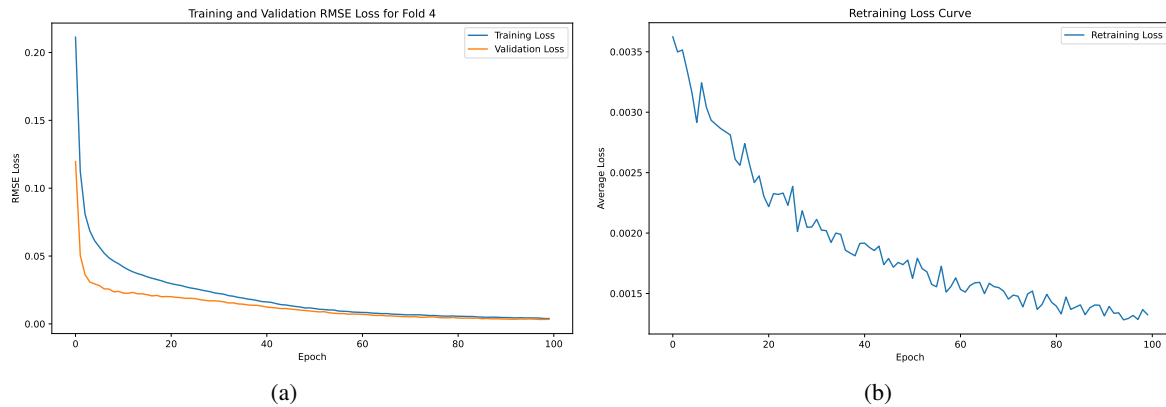


Figure 5: Visualization of the training-validation losses during (a) a representative training (fold 3) and (b) retraining with the whole data.

Multiple parameters contribute to Normalized average response, extending beyond vertical transformation, as evidenced by differing top and bottom plans. Additionally, the height of the building does not necessarily correlate with this value.

4. Conclusion

To help the designers' choices during the early phase of the project of tall buildings with outer diagrids, an AI-based workflow has been proposed. The considered building forms include ten geometrical features, such as the number of polygon sides for the top/bottom floors, the inter-storey height, the number of stories and the vertical transformations along the building height. Tunable parameters control the curvilinearity, tapering, and twisting of the base form. A surrogate model, using a MIMO-FNN, has been trained from a database of 1000 tall buildings with outer diagrids subjected to linear time-history lateral loading due to seven moderate earthquakes.

As 91 structural and economic/environmental responses, such as maximum overall acceleration, displacement, inter-story drift, von Mises stress, torsion, base shear force, base bending moment, total building mass, embodied carbon, and total cost are taken into account, the resulting surrogate model can be used in the early stages of the design of tall buildings to assist designers' choices. It is important to note that this study considers the maximum structural responses, so the surrogate model can predict the maximum responses but not their specific locations or time steps. This limitation was outside the scope of the current research. Future studies could focus on the time-history structural responses for all structural members to train a more comprehensive surrogate model, incorporating more detailed information from each tall building model. In the future, the database can be enriched with additional features and responses, and optimization tools can be applied to explore regions of interest in the design space and identify efficient designs. It would be relatively simple, as example, to use the MIMO-FNN together with an optimizer to achieve the goal of generating solutions alternative to those already in the database.

References

- [1] C. Preisinger, "Linking Structure and Parametric Geometry," *Architectural Design*, vol. 83, Mar. 2013. DOI: 10.1002/ad.1564.

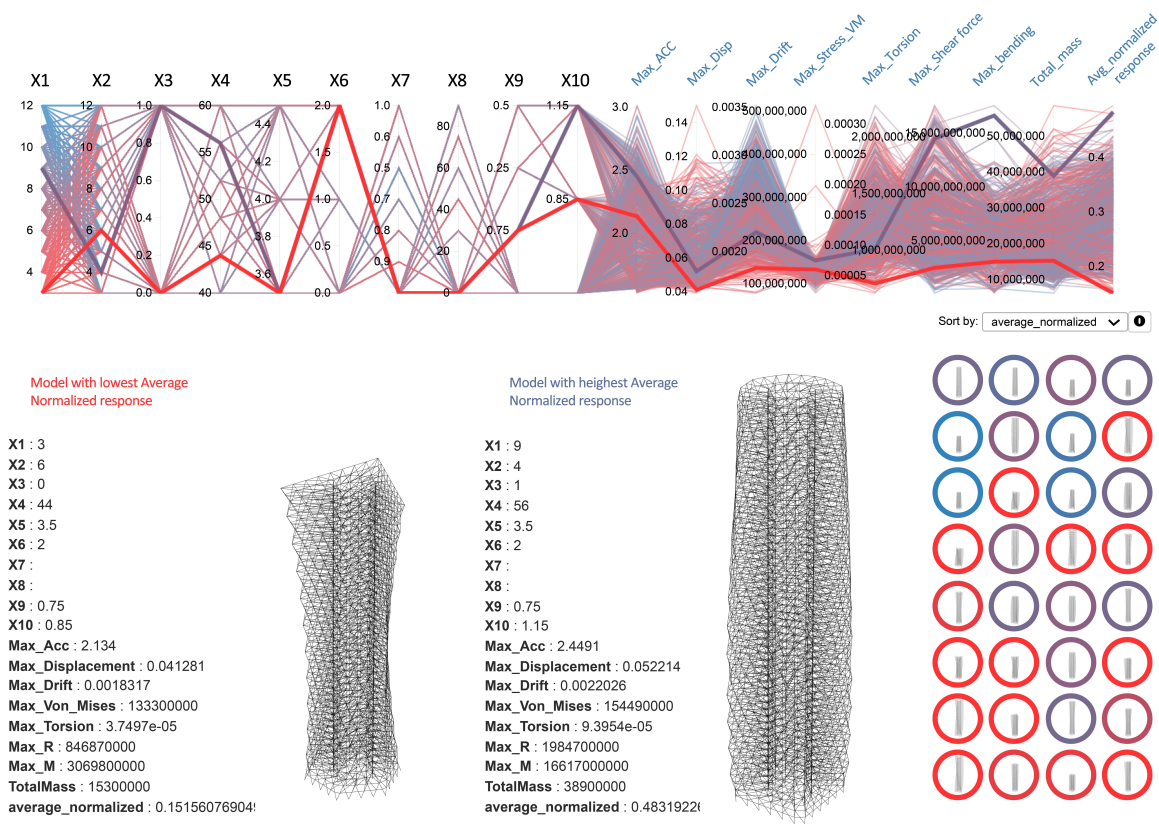


Figure 6: Top row: (red) best and (purple) worst building models according to the average normalized response. Features are represented on the right in black colour; responses are on the left in blue colour. Bottom row: (left) best and (center) worst model with the corresponding features/responses; (right) some of the remaining models.

- [2] E. Asadi, A. M. Salman, and Y. Li, “Multi-criteria decision-making for seismic resilience and sustainability assessment of diagrid buildings,” *Engineering Structures*, vol. 191, pp. 229–246, 2019, ISSN: 0141-0296. DOI: <https://doi.org/10.1016/j.engstruct.2019.04.049>.
- [3] M. Turrin, P. von Buelow, and R. Stouffs, “Design explorations of performance driven geometry in architectural design using parametric modeling and genetic algorithms,” *Advanced Engineering Informatics*, vol. 25, no. 4, pp. 656–675, 2011, Special Section: Advances and Challenges in Computing in Civil and Building Engineering, ISSN: 1474-0346. DOI: <https://doi.org/10.1016/j.aei.2011.07.009>.
- [4] T. D. Akinosho *et al.*, “Deep learning in the construction industry: A review of present status and future innovations,” *Journal of Building Engineering*, vol. 32, p. 101 827, 2020, ISSN: 2352-7102. DOI: <https://doi.org/10.1016/j.jobe.2020.101827>.
- [5] B. Ekici, Z. T. Kazanasmaz, M. Turrin, M. F. Tasgetiren, and I. S. Sariyildiz, “Multi-zone optimisation of high-rise buildings using artificial intelligence for sustainable metropolises. part 2: Optimisation problems, algorithms, results, and method validation,” *Solar Energy*, vol. 224, pp. 309–326, 2021, ISSN: 0038-092X. DOI: <https://doi.org/10.1016/j.solener.2021.05.082>.

- [6] H. Luo and S. G. Paal, “Artificial intelligence-enhanced seismic response prediction of reinforced concrete frames,” *Advanced Engineering Informatics*, vol. 52, p. 101 568, 2022, ISSN: 1474-0346. DOI: <https://doi.org/10.1016/j.aei.2022.101568>.
- [7] S. R. Vadyala, S. N. Betgeri, J. C. Matthews, and E. Matthews, “A review of physics-based machine learning in civil engineering,” *Results in Engineering*, vol. 13, p. 100 316, 2022, ISSN: 2590-1230. DOI: <https://doi.org/10.1016/j.rineng.2021.100316>.
- [8] P. Kazemi, A. Ghisi, and S. Mariani, “Classification of the Structural Behavior of Tall Buildings with a Diagrid Structure: A Machine Learning-Based Approach,” *Algorithms*, vol. 15, 10 2022, ISSN: 19994893. DOI: [10.3390/a15100349](https://doi.org/10.3390/a15100349).
- [9] P. Kazemi, A. Entezami, and A. Ghisi, “Machine learning techniques for diagrid building design: Architectural–Structural correlations with feature selection and data augmentation,” *Journal of Building Engineering*, vol. 86, p. 108 766, 2024, ISSN: 2352-7102. DOI: <https://doi.org/10.1016/j.jobbe.2024.108766>.
- [10] H.-T. Thai, “Machine learning for structural engineering: A state-of-the-art review,” *Structures*, vol. 38, pp. 448–491, 2022, ISSN: 2352-0124. DOI: <https://doi.org/10.1016/j.istruc.2022.02.003>.
- [11] H. Sun, H. V. Burton, and H. Huang, “Machine learning applications for building structural design and performance assessment: State-of-the-art review,” *Journal of Building Engineering*, vol. 33, p. 101 816, 2021, ISSN: 2352-7102. DOI: <https://doi.org/10.1016/j.jobbe.2020.101816>.
- [12] H. Zhang and Y. Huang, “Machine Learning Aided 2D-3D Architectural Form Finding at High Resolution,” in *CDRF 2020, Proceedings of the 2020 DigitalFUTURES*, 2021, pp. 159–168. DOI: https://doi.org/10.1007/978-981-33-4400-6_15.
- [13] D. Scaramozzino, B. Albitos, G. Lacidogna, and A. Carpinteri, “Selection of the optimal diagrid patterns in tall buildings within a multi-response framework: Application of the desirability function,” *Journal of Building Engineering*, vol. 54, p. 104 645, 2022, ISSN: 2352-7102. DOI: <https://doi.org/10.1016/j.jobbe.2022.104645>.
- [14] I. Aizenberg and C. Moraga, “Multilayer Feedforward Neural Network Based on Multi-valued Neurons (MLMVN) and a Backpropagation Learning Algorithm,” *Soft Computing*, vol. 11, pp. 169–183, 2007. DOI: <https://doi.org/10.1007/s00500-006-0075-5>.
- [15] R. Alizadeh, J. K. Allen, and F. Mistree, “Managing computational complexity using surrogate models: A critical review,” *Research in Engineering Design*, vol. 31, pp. 285–298, 2020. DOI: <https://doi.org/10.1007/s00163-020-00336-7>.
- [16] F. McKenna, M. H. Scott, and G. L. Fenves, “Nonlinear finite-element analysis software architecture using object composition,” *Journal of Computing in Civil Engineering*, vol. 24, pp. 95–107, 2010. DOI: [https://doi.org/10.1061/\(ASCE\)CP.1943-5487.0000002](https://doi.org/10.1061/(ASCE)CP.1943-5487.0000002).
- [17] Pacific Earthquake Engineering Research Center. “PEER Ground Motion Database.” (2024), [Online]. Available: <https://ngawest2.berkeley.edu/>.
- [18] E. Junda, C. Málaga-Chuquitaype, and K. Chawgien, “Interpretable machine learning models for the estimation of seismic drifts in CLT buildings,” *Journal of Building Engineering*, vol. 70, p. 106 365, 2023, ISSN: 2352-7102. DOI: <https://doi.org/10.1016/j.jobbe.2023.106365>.



Copyright Declaration

Before publication of your paper in the Proceedings of the IASS Annual Symposium 2024, the Editors and the IASS Secretariat must receive a signed Copyright Declaration. The completed and signed declaration may be uploaded to the EasyChair submission platform or sent as an e-mail attachment to the symposium secretariat (papers@iass2024.org). A scan into a .pdf file of the signed declaration is acceptable in lieu of the signed original. In the case of a contribution by multiple authors, either the corresponding author or an author who has the authority to represent all the other authors should provide his or her address, phone and E-mail and sign the declaration.

Paper Title:

Deep learning approach to structural performance prediction of tall buildings in seismic areas

Author(s):

Pooyan KAZEMI (a), Michela TURRIN (b), Charalampos ANDRIOTIS (b), Alireza ENTEZAMI (a), Aldo GHISI (a), Stefano MARIANI (a)

Affiliation(s):

(a) Department of Civil and Environmental Engineering, Politecnico di Milano Piazza Leonardo da Vinci 32, 30133, Milano, Italy

(b) Architectural Engineering and Technology Department, Delft University of Technology, Julianalaan 134, 2628 BL, Delft, The Netherlands

Address:

Politecnico di Milano, Piazza Leonardo da Vinci 32, 30133, Milano, Italy

Phone:

+393518018836

E-mail:

seyedpooyan.kazemi@polimi.it

I hereby license the International Association for Shell and Spatial Structures to publish this work and to use it for all current and future print and electronic issues of the Proceedings of the IASS Annual Symposia. I understand this licence does not restrict any of the authors' future use or reproduction of the contents of this work. I also understand that the first-page footer of the manuscript is to bear the appropriately completed notation:

Copyright © 2024 by <name(s) of all of the author(s)>

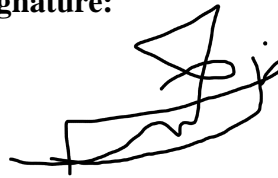
Published by the International Association for Shell and Spatial Structures (IASS) with permission

If the contribution contains materials bearing a copyright by others, I further affirm that (1) the authors have secured and retained formal permission to reproduce such materials, and (2) any and all such materials are properly acknowledged by reference citations and/or with credits in the captions of photos/figures/tables.

Printed name:

Pooyan Kazemi

Signature:

A handwritten signature in black ink, appearing to be 'Pooyan Kazemi', written over a horizontal line.

Location:

Milan

Date:

01.07.2024